

In this case, the filter coefficients are calculated by equation (16).

$$C_{ij}(n+1, k) = C_{ij}(n, k) + \mu f(s_i(n))g(s_j(n-k)), k \in [0, L] \quad (16)$$

where μ is the learning rate.

When the two output signals are independent, then filter coefficients will convergence. We extend this rule to the separation method of non-stationary signals. For calculation simplicity, in the algorithm, nonlinear function is set as

$$f = (\cdot)^3, g = (\cdot) \quad (17a, b)$$

The effect of other source signals to mixtures is eliminated by the estimated filter, and the estimates of non-stationary source signals are obtained. But as the coupling between the signals at the same time point, each simultaneous output equations are used to further eliminate the coupling between the signals, and each point of non-stationary signals are estimated.

In the case of two sources, from equation (9), we can obtain

$$s_i(n) = x_i(n) - C_{ij}(n, 0) \cdot s_j(n) - \sum_{k=1}^L C_{ij}(n, k) \cdot s_j(n-k), i, j \in (1, 2), i \neq j \quad (18)$$

From equations (18), we can get $s_1(n)$ and $s_2(n)$, then

$$\begin{bmatrix} 1 & C_{12}(n, 0) \\ C_{21}(n, 0) & 1 \end{bmatrix} \begin{bmatrix} s_1(n) \\ s_2(n) \end{bmatrix} = \begin{bmatrix} x_1(n) \\ x_2(n) \end{bmatrix} - \begin{bmatrix} \sum_{k=1}^L C_{12}(n, k) \cdot s_2(n-k) \\ \sum_{k=1}^L C_{21}(n, k) \cdot s_1(n-k) \end{bmatrix} \quad (19)$$

Thus the output of the system is available.

$$\begin{bmatrix} s_1(n) \\ s_2(n) \end{bmatrix} = \begin{bmatrix} 1 & C_{12}(n, 0) \\ C_{21}(n, 0) & 1 \end{bmatrix}^{-1} \times \left(\begin{bmatrix} x_1(n) \\ x_2(n) \end{bmatrix} - \begin{bmatrix} \sum_{k=1}^L C_{12}(n, k) \cdot s_2(n-k) \\ \sum_{k=1}^L C_{21}(n, k) \cdot s_1(n-k) \end{bmatrix} \right) \quad (20)$$

So we can get the program flow of the algorithm, which is shown in figure 2.

The main steps of the algorithm are as follows:

- Step 1: Initialize the filter coefficients and the learning rate;
- Step 2: Starting from point 2, calculate the source signal value of point n;
- Step 3: According to the previous value, calculate the gain of the filter coefficients;
- Step 4: Calculate filter coefficients;
- Step 5: if $k < \text{signal length}$, return to step 2.

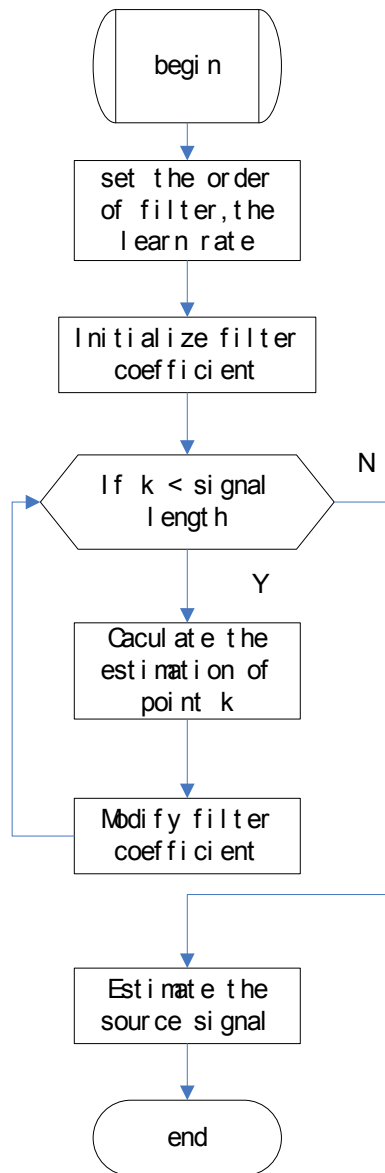


Figure 2. Program flow of the algorithm

V. SIMULATIONS

This section uses mechanical vibration simulation signals as non-stationary signal sources; the separation performance of the blind source separation algorithm for convolution mixture of non-stationary signals is researched.

Three signals are used to test the algorithm. s_1 is a FM sine signals. s_2 is a non-stationary source signals with the frequency mutations in the signal. s_3 is a sine signal.

$$\begin{aligned}
 s1 &= \sin(500\pi t + 5 \sin(6\pi t)) \\
 s2 &= \begin{cases} \sin(74\pi t), & 0 \leq t \leq t_1 \\ \sin(40\pi t), & t_1 < t \leq t_2 \end{cases} \\
 s3 &= \sin(240\pi t)
 \end{aligned} \tag{21}$$

They are mixed by equation (3), in which the filter coefficients are

$$\begin{aligned}
 A_{12} &= [-0.0464 \quad -0.4099 \quad -0.1922 \quad -0.1166 \quad 0.0725]^T \\
 A_{13} &= [-0.2709 \quad 0.1981 \quad -0.1720 \quad 0.4294 \quad -0.2702]^T \\
 A_{21} &= [-0.4079 \quad 0.0543 \quad -0.3843 \quad 0.2910 \quad -0.2804]^T \\
 A_{23} &= [-0.3221 \quad -0.1987 \quad -0.0426 \quad -0.3498 \quad -0.0382]^T \\
 A_{31} &= [0.1424 \quad 0.3732 \quad -0.1940 \quad 0.1063 \quad -0.2582]^T \\
 A_{32} &= [0.2023 \quad -0.4758 \quad 0.4293 \quad -0.0237 \quad -0.0284]^T
 \end{aligned} \tag{22}$$

The waveforms of source signals, mixed signals and separated signals in the time domain are shown in figure 3. Sampling length is 4096. s_1, s_2, s_3 are source signals. x_1, x_2, x_3 are mixtures. ss_1, ss_2, ss_3 are the separated signals. The waveform between 2.3 seconds and 2.85 seconds is shown in figure 3, which covers the point of the frequency mutation in the signal s_2 . It can be seen that the separated signal waveforms are very similar with the source signal waveforms.

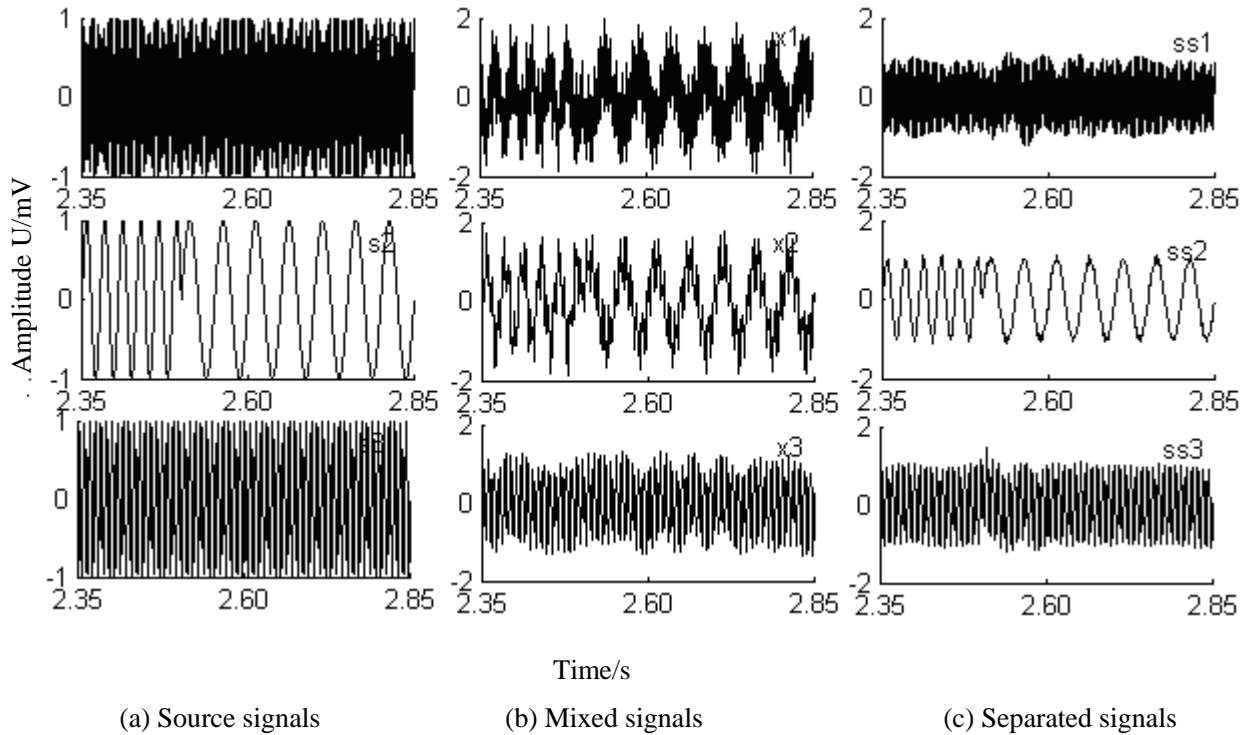


Figure 3. Waveforms of simulation signals in time domain

To show the result more obvious, short time fourier transform (STFT) is used to represent the signal frequency characteristics. STFT spectrums of source signals, mixed signals and separated signals are shown in figure 4. It can be seen from figure 4 that early in the separation process, three signals have a strong coupling phenomenon, as time passed, weaker coupling exists in signals, which indicates that the asymptotic convergence of the iterative process. In the vicinity of 2.5 seconds, source 1 and source 3 have been completely separated, but the effect on source 2 from source 1 and source 3 has not completely eliminated. From the waveforms in figure 3 and scale in figure 4, the effect is in fact very small. The impact on source 1 and source 3 is relatively large near the frequency mutations of source 2. After almost 0.2 second iterative process, the effect on source 1 and source 3 from source 2 is completely eliminated, that indicates the source signals are well separated. Simulation results show that the method is effective for non-stationary signals.

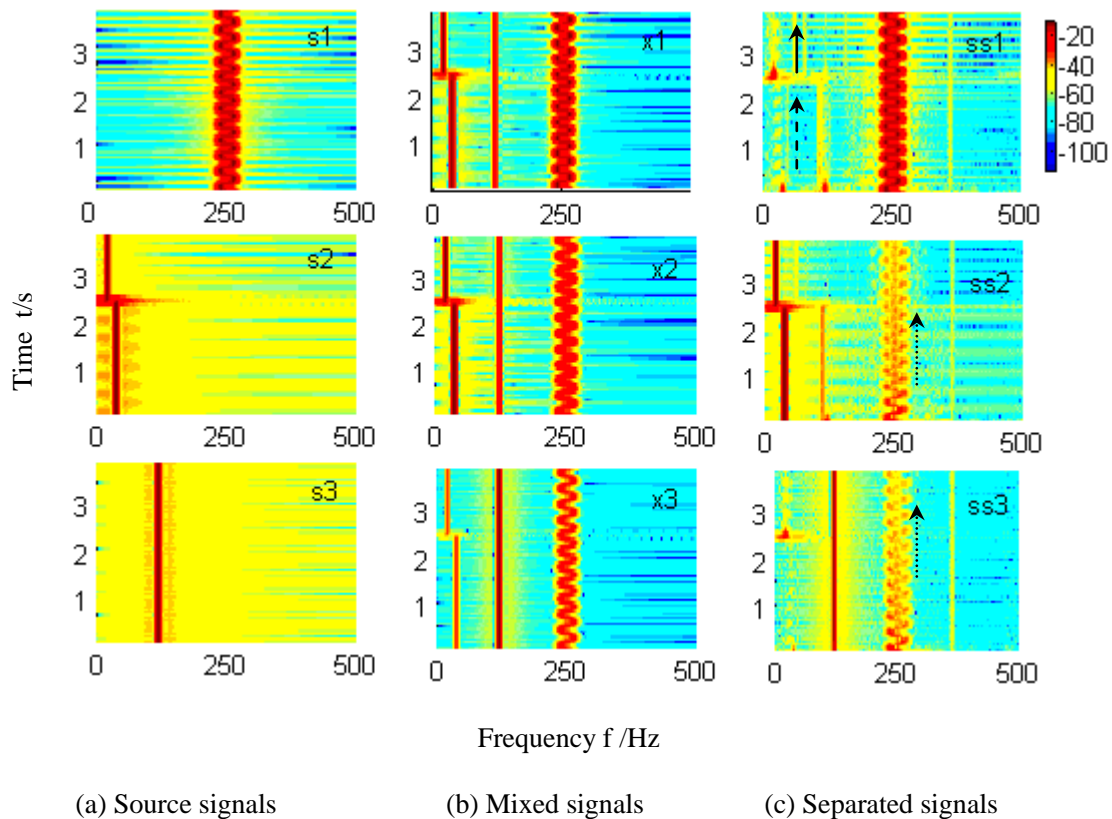


Figure 4. STFT spectrum of simulation signals

The iterative process of the filter coefficients is shown in figure 5. The filter coefficients fluctuate when the frequency mutates. The filter coefficients are gradually convergence in the iteration without frequency mutation.

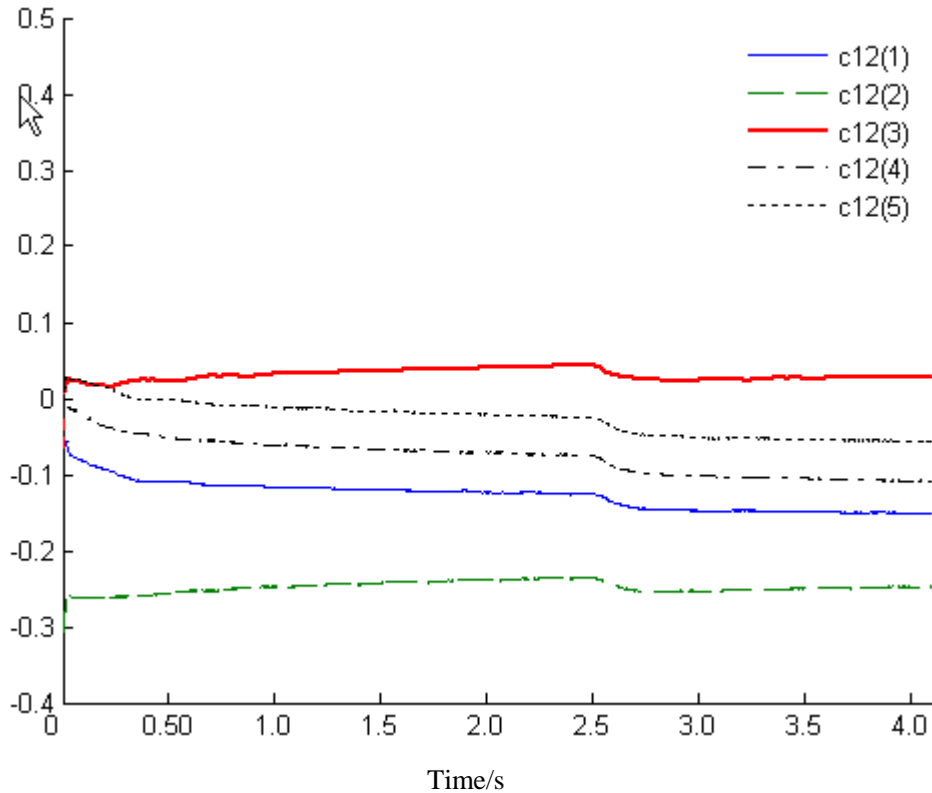


Figure 5. The iterative process of the filter coefficients in simulation

VI. EXPERIMENTS

Simulation results show that the algorithm is valid for non-stationary signals. In this section, the research is carried out to test the algorithm with non-stationary mechanical vibration. The mechanical vibration signals are obtained from the test-bed on the body of two electromotor. The test system is shown in figure 6. Piezoelectric sensors are installed on the chassis to collect mechanical vibration signals. One of the electromotor is 750W (electromotor 1), and another one is 2.2kW (electromotor 2). Two sensors are set on the top of electromotor 1 (sensor 1) and electromotor 2 (sensor 2), and one on the board (sensor 3). The rotating speed of the electromotor 2 is controlled by the inverter frequency control to obtain non-stationary vibration signals. The

rotating speed of the electromotor 1 is uniform. The test-bed is used to simulate such situations in the factory: multi rotating machineries are operating at the same time; the vibration signals from each machine are mixed with the vibration signals from other machines, even with the noise.



Figure 6. Test system

PCL-1800 data acquisition card is used to data acquisition. Structural principle of the test system is shown in figure 7.

The rotation frequency of the electromotor in the test system is 25Hz. PCL-1800 is a high-speed communication card which is compatible with ISA bus. A 12 bit A/D chip with high performance, wide dynamic range, excellent resistance to noise and low power consumption is used to complete A/D conversion. The card also come with high-performance with 1K byte FIFO to reduce CPU load, with 16 single-ended or 8 differential analog inputs, 2-port 12 bits D/A output, 16-port digital inputs, 16-port digital outputs and a 16-port counter channel. The PCL-1800 has four kinds of data communication ways. The performances of each kind of communication ways

are shown in table 1.

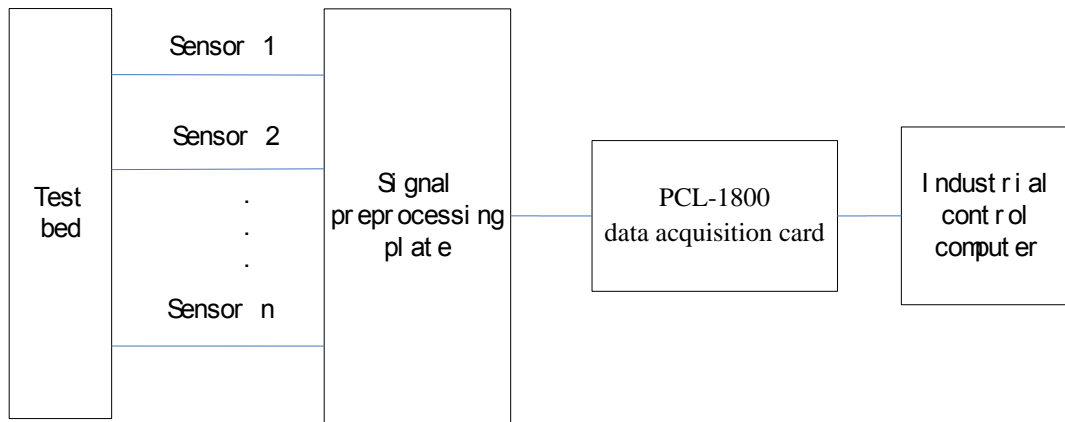


Figure 7. Structural principle of the test system

Table 1: The performance data communication ways of PCL-1800[23]

Data communication ways	A/D speed
Software query	10~20KHz
Interrupt	10~30KHz
DMA	200KHz
FIFO	330KHz

In the program of multi-port data acquisition, the interrupt data communication way is used to data acquisition. The sampling data are read by means of FIFO. The flow of data acquisition is shown in figure 8.

The measurements of electromotor vibration are used as vibration source signal when they run individually, which are shown in figure 9. The vibration signal measured from sensor 1 when only electromotor 1 run is denoted as source signal s_1 . The vibration signal measured from sensor 2 when only electromotor 2 run is denoted as source signal s_2 . The STFT spectrums of source signals are shown in figure 10. The arrow point in figure 10 shows the change point of the rotating frequency of electromotor 2.

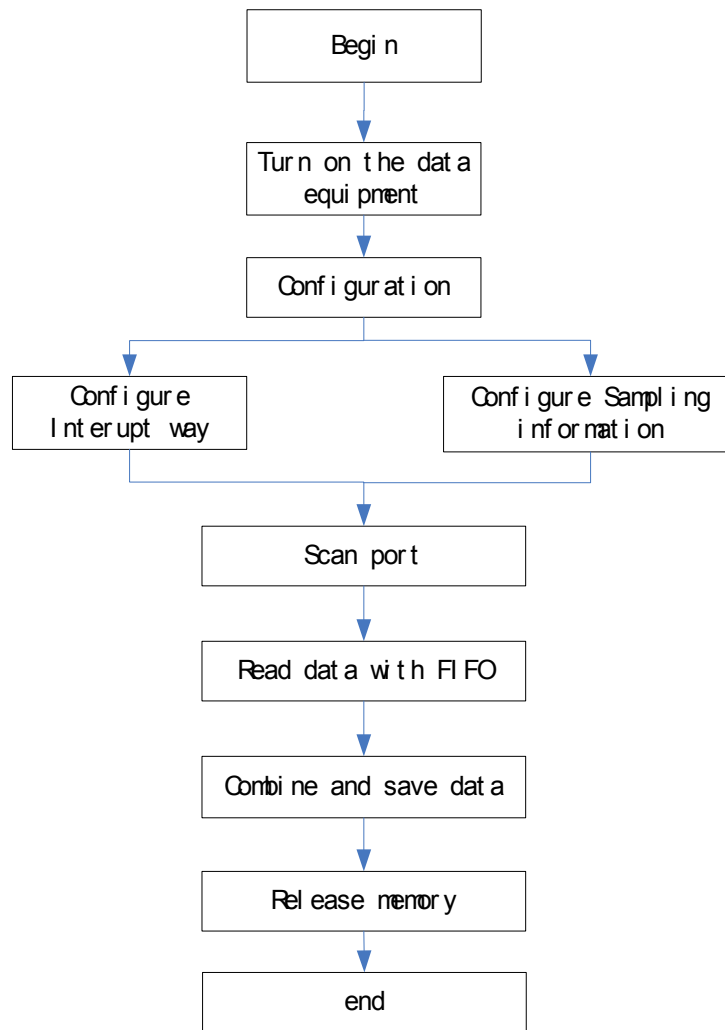
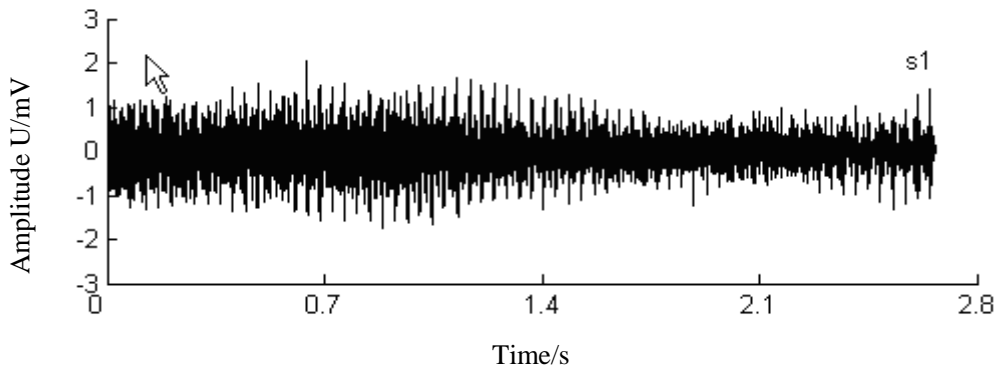
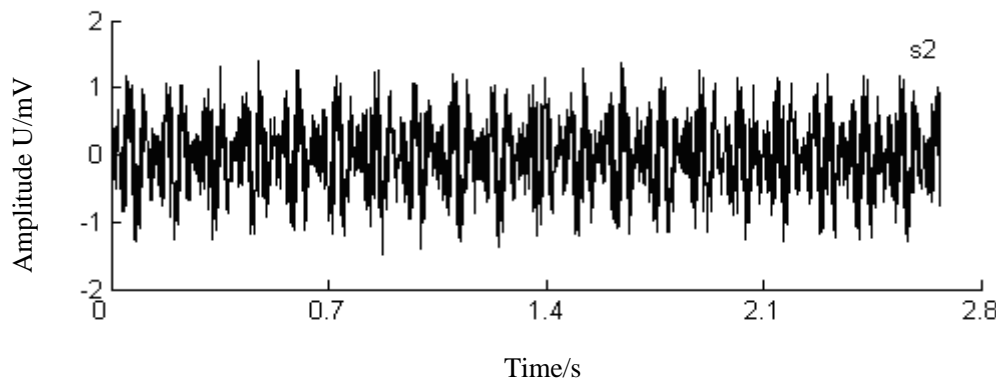


Figure 8. The flow of data acquisition

The measurements are used as mixtures as two electromotor run together, which are shown in figure 11. The vibration signal measured from sensor 1 when two electromotor run together is denoted as mixture signal x_1 . The vibration signal measured from sensor 2 is denoted as mixture signal x_2 . The vibration signal measured from sensor 3 is denoted as mixture signal x_3 . The STFT spectrums of mixture signals are shown in figure12. It can be seen from figure 12, the electromotor 2 has greater effect on the mixture signal x_1 and x_3 , and the effect of electromotor 1 on the mixture signal x_2 is weak.

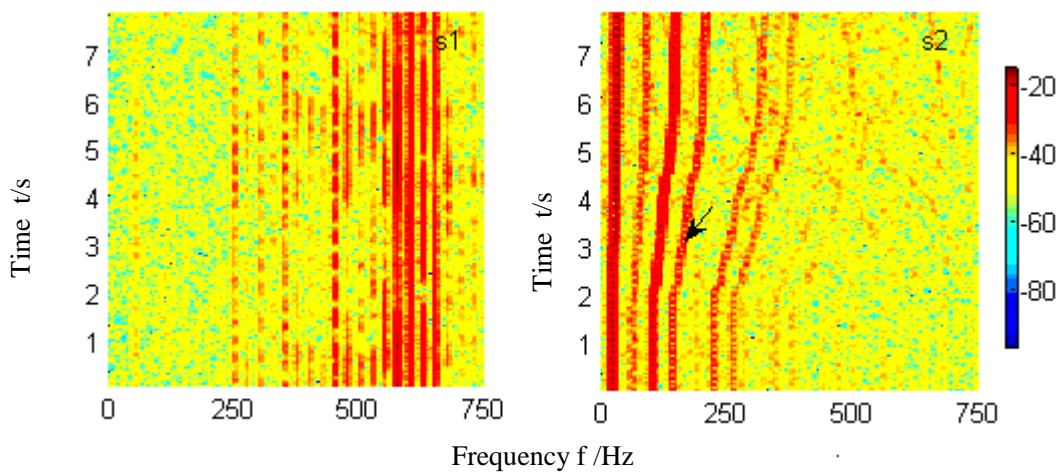


(a) Electromotor 1



(b) Electromotor 2

Figure 9. Waveforms of source signals in time domain



(a) Electromotor 1

(b) Electromotor 2

Figure 10. STFT spectrum of source signals

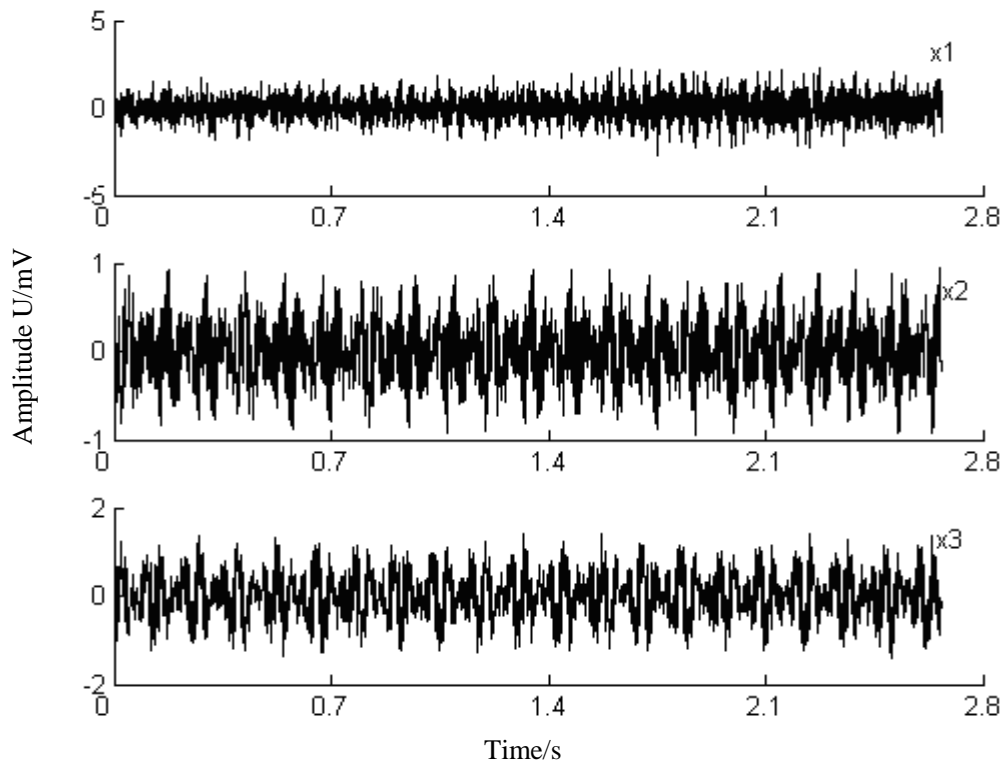


Figure 11. Waveforms of mixed signals in time domain

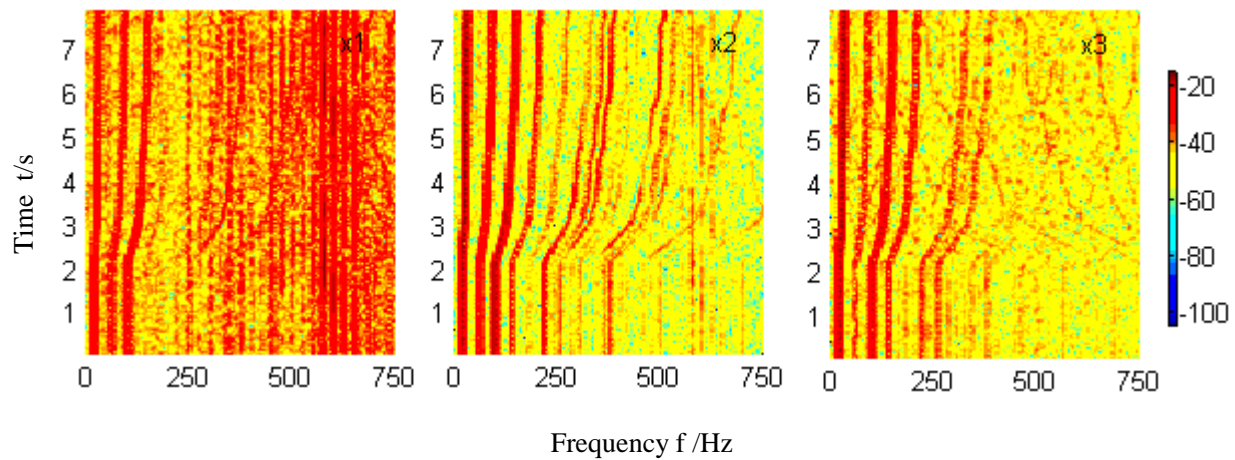


Figure 12. STFT spectrum of mixed signals

In this test, what we concerned is the separation performance, so the physics meaning of the value of the spectrum is not specified. The algorithm is used to separate the measurements to get the estimation source signals, which are denoted as ss_1 , ss_2 and ss_3 . The waveforms of separated

signals in time domain are shown in figure 13. The STFT spectrums of source signals, mixture signals and separated signals are shown in figure14.

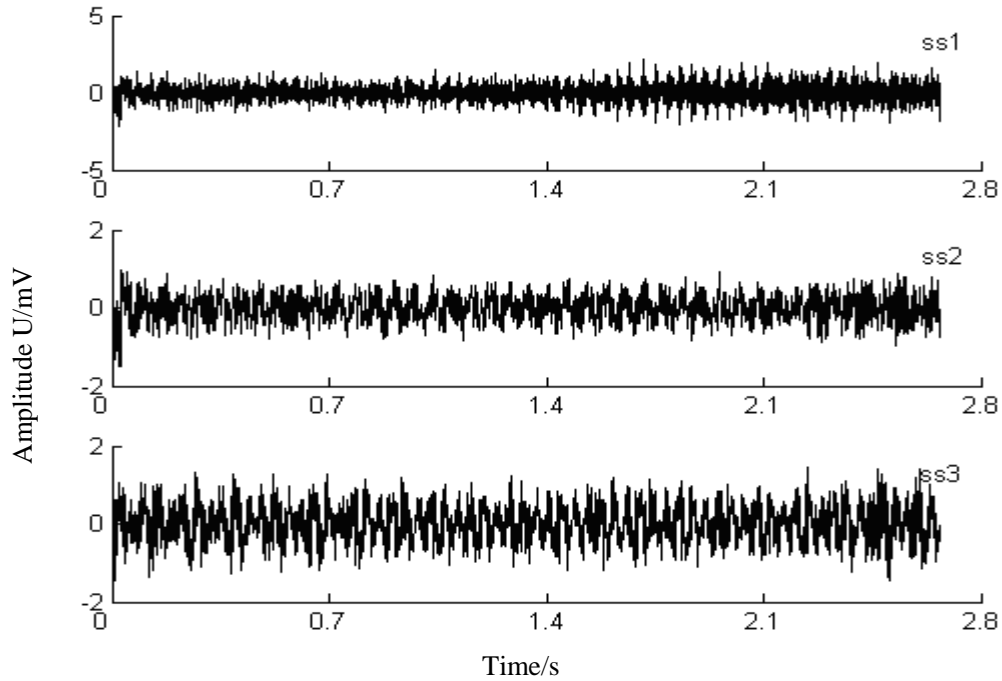


Figure 13. Waveforms of separated signals in time domain

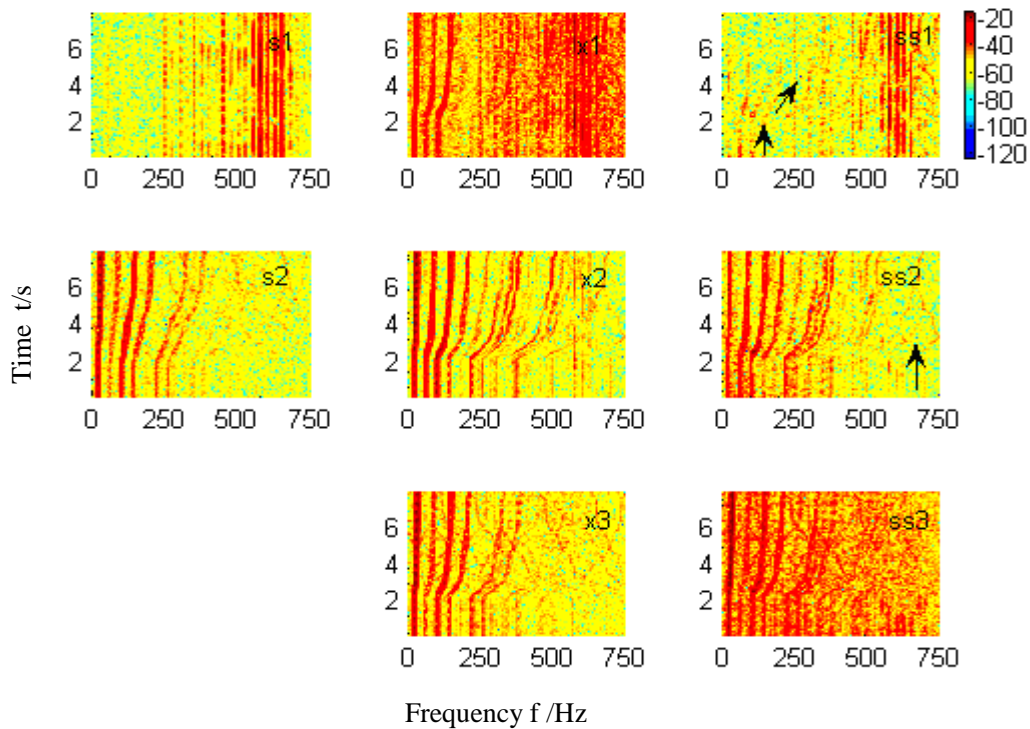


Figure 14. STFT spectrum of the signals

Compared figure 9 with figure 13, it can be seen that $ss1$ is similar to $s1$, and $ss2$ is similar to $s2$ in time domain. Which illustrate that $ss1$ is corresponding to the vibration signal of electromotor 1, and $ss2$ is corresponding to the vibration signal of electromotor 2. The arrow points on the spectrum of separated signal $ss1$ show the gradual separation process of the non-stationary signals. Although some lines do not get completely separate, the interaction is weak between signals by comparing source signals with mixture signals and separated signals. The two source signals are well separated.

The iterative process of the filter coefficients is shown in Figure 15. The filter coefficients fluctuate slightly with the signal frequency and gradually tend to be stable as the iterative process proceeding.

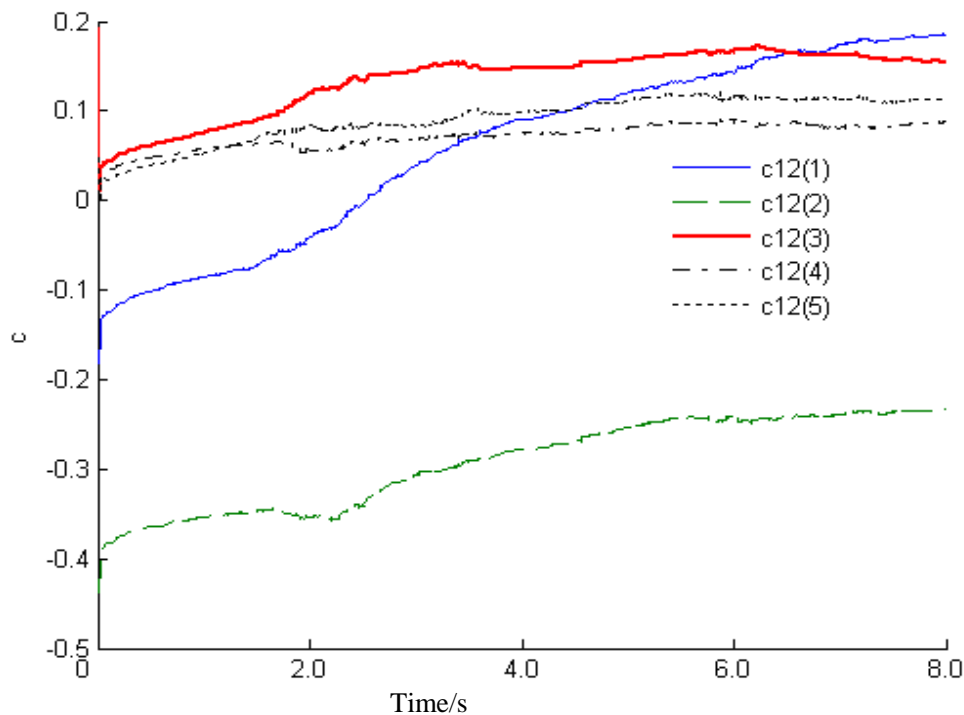


Figure 15. The iterative process of the filter coefficients in experiment

VII. CONCOLUTIONS

From the simulation experiment, the non-stationary convolutive mixed signal separation algorithm has good separation performance. The experiments on non-stationary mechanical vibration signal show that the algorithm can well separate different mechanical vibration signals.

Therefore, further study of the algorithm in gearbox fault diagnosis is worthy to carry out to eliminate non-stationary signals from another machine on the mechanical vibration of the gearbox, and to improve the accuracy of diagnostic methods. At the same time, the algorithm can also be extended to non-stationary internal gearbox vibration signal separation, provide a basis for precise fault position.

ACKNOWLEDGEMENTS

This paper is supported by the National Natural Science Foundation of China (50905050).

REFERENCES

- [1] A. Ypma, "Learning Methods for Machine Vibration Analysis and Health Monitoring", Doctor of Engineering thesis, Pattern Recognition Group, Dept. of Applied Physics, Delft University of Technology, Netherlands, 1998.
- [2] Z. N. Li, W. B. Liu and X. B. YI, "Underdetermined Blind Source Separation Method of Machine Faults Based on Local Mean Decomposition", Chinese Journal of Mechanical Engineering, Vol. 47, No.7, pp. 97-102, Apr. 2011.
- [3] W. F. Wu, X. H. Chen and X. J. SU, "Blind Source Separation of Single-channel Mechanical Signal Based on Empirical Mode Decomposition", Chinese Journal of Mechanical Engineering, Vol. 47, No.4, pp. 12-16, Apr. 2011.
- [4] G. Colas, "Blind Source Separation: a Tool for Rotating Machine Monitoring by Vibration Analysis" International Journal of Sound and Vibration, Vol. 248, No.5, pp. 865-885, Dec. 2001.
- [5] G. Guillaume and S. Christine, "Blind Source Separation: A New Pre-Processing Tool for Rotating Machines Monitoring"? IEEE Transactions on Instrumentation and Measurement, Vol. 52, No.3, pp. 790-795, June. 2003.
- [6] H. X. Ye, S. X. Yang and J. X. Yang, "Temporal Blind Source Separation Algorithm for Convolution Mixtures with Multi Vibration Sources", Chinese Journal of Mechanical Engineering, Vol. 45, No. 1, pp.189-194,199, Jan. 2009.

- [7] M. Parvaix and L. Girin, "Informed Source Separation of Linear Instantaneous Under-Determined Audio Mixtures by Source Index Embedding", *IEEE Transactions on Audio, Speech and Language Processing*, Vol. 19, No. 6, pp. 1721-1733, Aug. 2011.
- [8] P. Tichavsky and Z. Koldovsky, "Weight Adjusted Tensor Method for Blind Separation of Underdetermined Mixtures of Nonstationary Sources", *IEEE Transactions on Signal Processing*, Vol. 59, No. 3, pp. 1037-1047, Mar. 2011.
- [9] D. Farina, M. F. Lucas and C. Doncarli, "Optimized Wavelets for Blind Separation of Nonstationary Surface Myoelectric Signals", *IEEE Transactions on Biomedical Engineering*, Vol. 55, No. 1, pp. 78-86, Jan. 2008.
- [10] R. Guidara, S. Hosseini and Y. Deville, "Blind Separation of Nonstationary Markovian Sources Using an Equivariant Newton–Raphson Algorithm", *IEEE Signal Processing Letters*, Vol. 16, No. 5, pp. 426-429, May. 2009.
- [11] H. Rimminen, J. Lindstrom and R. Sepponen, "Positioning Accuracy and Multi-Target Separation With a Human Tracking System Using Near Field Imaging", *International Journal on Smart Sensing and Intelligent Systems*, Vol. 2, No.1, pp. 156–175, Mar. 2009.
- [12] B. Makkiabadi, D. Jarchi and S. Sanei, "A New Time Domain Convolutional BSS of Heart and Lung Sounds, Acoustics", *IEEE International Conference on Speech and Signal Processing (ICASSP)*, Vol. 25-30, pp. 605 – 608, Mar. 2012, Kyoto, Japan.
- [13] G. P. Cedric, C. Marco and C. Brunner, C. Jutten and P. Gert, "Nonstationary Brain Source Separation for Multiclass Motor Imagery", *IEEE Transactions on Biomedical Engineering*, Vol. 57, No. 2, pp.469-478, Feb. 2010.
- [14] S. Choi and A. Cichocki, "Blind Separation of Nonstationary Sources in Noisy Mixtures", *International Journal of Electronics Letters*, Vol. 36, No.9, pp. 848-849, Apr. 2000.
- [15] T. Ishibashi, K. Inoue and H. Gotanda, "Studies on Estimation of the Sources Number in Blind Source Separation Problems", *International Joint Conference SICE-ICASE*, pp. 5169-5174, Oct. 2006, Busan, Korea.
- [16] N. Pan, X. Wu and Y. L. Chi, X. Q. Liu and C. Liu, "Machine Fault Diagnosis Based on Frequency-Domain Blind Deconvolution". *Proceedings of 2011 International Conference on Modeling, Identification and Control*, pp. 63-68, June. 2011, Shanghai, China.

- [17] Y. Y. Na and J. Yu, "Kernel and Spectral Methods for Solving the Permutation Problem in Frequency Domain BSS", WCCI 2012 IEEE World Congress on Computational Intelligence, pp.1-8, June. 2012, Brisbane, Australia.
- [18] S. M. Naqvi, Y. Zhang, T. Tsalaile, S. Saneiz and J. A. Chambers, "Evaluation of Emerging Frequency Domain Convolutional Blind Source Separation Algorithms Based on Real Room Recordings", 5th IEEE Sensor Array and Multichannel Signal Processing Workshop, pp. 345 - 348, July. 2008, Darmstadt, Germany.
- [19] T. T. Liu, X. M. Ren, "A Blind De-convolution Technique for Machine Fault Diagnosis", 2009 Second International Conference on Information and Computing Science", pp. 232-235, May. 2009, Manchester, England, UK.
- [20] I. Russell, J. T. Xi and A. Mertins, "Blind Source Separation of Nonstationary Convolutionally Mixed Signals in the Subband Domain", IEEE International Conference on Acoustics, Speech, and Signal Processing (ICASSP), Vol. 5, pp. 481-484, May. 2004, Quebec, Canada.
- [21] S. B. Han, J. Cui and P. Li, "Post-processing for Frequency-domain Blind Source Separation in Hearing Aids", 7th International Conference on Information, Communications and Signal Processing, pp. 1 – 5, 8-10, Dec. 2009, Beijing, China.
- [22] T. Nguyen and C. Jutten, "Blind Source Separation for Convolutional Mixtures", IEEE Transactions on Signal Processing, Vol. 45, No. 2, pp. 209-229, July. 1995.
- [23] Advantech CO. LTD, PCL-1800 Manual, 2005.